Thin-Film Deposition of Organic−Inorganic Hybrid Materials

David B. Mitzi*

IBM T. J. Watson Research Center, P.O. Box 218, Yorktown Heights, New York 10598

Received February 9, 2001. Revised Manuscript Received April 13, 2001

Organic−inorganic hybrid films present special challenges and opportunities with respect to potential applications, as well as for the observation of interesting physical phenomena. Although the often disparate characteristics (e.g., solubility and thermal stability) of the two components provide a potential barrier toward forming workable and convenient film deposition strategies, recent results have demonstrated that not only is it possible to develop suitable techniques for these materials but relatively simple processes are often sufficient to yield high quality films. In the current review, some of these recent results on organic−inorganic hybrid films are discussed, with selected examples chosen from among the deposition of sol−gel materials, self-assembled hybrids, Langmuir−Blodgett films, and artificially layered materials. In addition to discussing film-deposition techniques, an effort will also be made, where appropriate, to indicate how the resulting films might be useful for applications such as organic−inorganic electronic or photonic devices.

I. Introduction

Organic−inorganic hybrids have attracted substantial attention because of the potential of combining distinct properties of organic and inorganic components within a single molecular composite. Organic materials offer structural flexibility, convenient processing, tunable electronic properties, photoconductivity, efficient luminescence, and the potential for semiconducting and even metallic behavior. Inorganic compounds provide the potential for high carrier mobilities, band gap tunability, a range of magnetic and dielectric properties, and thermal and mechanical stability. In addition to combining distinct characteristics, new or enhanced phenomena can also arise as a result of the interface between the organic and inorganic components. Electron-transfer processes at organic−inorganic interfaces have, for example, been examined.[1−3] Dielectric modulation in organic−inorganic systems has also led to enhanced binding energies for excitons in the inorganic framework of the structure, as a result of the smaller dielectric constant and reduced screening in the organic component of the hybrid.[4]

The self-assembling organic−inorganic perovskites[5] are one family of crystalline hybrids that provides a pathway to an alternating framework of semiconducting inorganic sheets and organic layers. The ability to control the thickness and metal/halogen content of the perovskite sheets and the chemical/physical properties of the organic cations (e.g., length, shape, and polarizability) provides a handle to tune the characteristics of the natural quantum well structures. Members of the hybrid perovskite family exhibit a semiconductor-metal transition as a function of increasing perovskite sheet thickness (or well width).[6,7] Room-temperature photoluminescence,[8,9] third harmonic generation,[10] and polariton absorption[11] arise from excitons, with exceptionally large binding energies and oscillator strength, in the inorganic sheets. A thin film heterostructure electroluminescent (EL) device has been demonstrated[12] employing $(C_6H_5C_2H_4NH_3)_2PbI_4$ as the active light-emitting component, with intense EL of more than 10 000 cd m^{-2} observed at liquid nitrogen temperature. Recently, the incorporation of a dye molecule within the perovskite framework[13] enabled the demonstration of room-temperature organic−inorganic light-emitting devices (LEDs).[14] The inorganic framework in these systems has a strong influence on the luminescence efficiency of the dye molecule, indicating the importance of interaction between the two components of the structure. Solution-processed organic−inorganic perovskites have also been employed as channels in thin-film field-effect transistors (TFTs), with mobilities of ∼1 cm^2/V sec.[15−17] In addition to the perovskite family, numerous other glasslike and crystalline organic−inorganic hybrids exhibit a range of interesting properties including superconducting transitions,[18] large second-harmonic generation efficiency,[19] and molecular recognition and catalytic properties.[20]

Many studies and potential applications involving the organic−inorganic hybrids depend on the availability of simple and reliable thin film deposition techniques. Deposition of hybrid materials is often challenging because of the distinctly different physical and chemical character of the organic and inorganic components. Organic materials, for example, tend to be soluble in different solvents than those appropriate for the inorganic framework, making solution deposition techniques (e.g., spin coating, stamping, and printing) generally impractical. For those cases where the hybrid is soluble, solution techniques are sometimes not appropriate because of adverse substrate wetting characteristics or

* To whom correspondence should be addressed. E-mail: dmitzi@us.ibm.com.

10.1021/cm0101677 CCC: $20.00
Published on Web 06/26/2001

the need to uniformly coat an irregular surface. With regard to vacuum evaporation techniques, the gradual heating of organic−inorganic composites typically results in the decomposition or dissociation of the organic component at a lower temperature than that required for evaporation of the inorganic component. Despite these apparent difficulties, organic−inorganic hybrids offer a number of important opportunities for thin film deposition. This review will provide a selected compilation of recent developments in this area, demonstrating that a number of simple and versatile techniques can be employed for the deposition of this important class of materials.

II. Solution Processing

One important method for processing hybrid films involves the use of sol−gel techniques, in which a solid phase forms through the gelation of a colloidal suspension.[21] The sol−gel process involves first preparing the "sol" (i.e., colloidal suspension) or solution containing the appropriate starting materials. In traditional sol−gel preparations, the sol is formed from a solution of metal alkoxides [$M^{n+}(OR)_n$] or colloidal particles of hydrous or anhydrous metal oxides. Although single component alkoxides can be used, one of the advantages of the sol−gel technique is that multiple components can be conveniently mixed in solution on the nanometer length scale, enabling the formation of homogeneous ceramics and glasses. In addition, the alkoxide precursors can readily be purified, leading to the potential for high purity products.

Although the term sol−gel implies starting the process with a sol (strictly speaking a colloidal suspension), often the starting point is more accurately a solution. In silica-based (SiO_2) preparations, for example, the commonly used tetraethyl orthosilicate (TEOS) alkoxide precursor is often dissolved in ethanol or a similar alcohol. Gelation of the sol is accomplished through the low-temperature hydrolysis and condensation (polymerization) reactions represented in Scheme 1 and initiated by the addition of water. The result of the condensation step is the formation of an extended metal oxide network. Organic−inorganic hybrid gels may be prepared by using mixtures of alkoxy groups, with some of the bonds being metal−oxygen bonds and some being metal−carbon bonds. The resulting hybrid gel or "ORMOCER" (organically modified ceramic) [also called "ORMOSIL" (organically modified silicate) or "CERAMER"] may have organic groups linked to a stiff inorganic backbone, or the organic and inorganic components may form an interpenetrating network.[22−24]

Scheme 1

Hydrolysis Reaction

$$(1)\quad M(OR)_n + x\,H_2O \rightarrow M(OH)_x(OR)_{n-x} + x\,ROH$$

Condensation Reactions

$$(2a)\quad \text{M-OR} + \text{M-OH} \rightarrow \text{M-O-M} + \text{R-OH}$$

$$(2b)\quad \text{M-OH} + \text{M-OH} \rightarrow \text{M-O-M} + \text{H-OH}$$

The sol−gel process can be used to create fibers, monolithic pieces, powders, or films of the resulting oxide ceramic. In the preparation of thin films, the sol is prepared in an appropriate solvent (e.g., various alcohols) and a controlled amount of water may be added to initiate the condensation reactions. The solutions chosen for thin film deposition are generally those that are fast gelling and drying, and they are applied to a substrate by standard solution-processing techniques (e.g., spin coating, dipping, or spaying). The condensation reactions, evaporation of solvent, and aggregation of species in the sol result in the formation of a gel film. The wet gel layer is transformed into a glass or ceramic through a low-temperature cure or anneal. In traditional sol−gel preparations, the heat treatments are designed to remove organic residuals and water through evaporation, pyrolysis, or combustion, as well as to provide densification. For the deposition of an organic−inorganic hybrid, care must be taken to heat the film below the decomposition point of the organic component. Also, the tendency of wet gel layers to crack during drying generally limits the thickness of the films to approximately $<1\ \mu$m.

Numerous examples of hybrid films produced using the sol−gel process have appeared recently, highlighting the versatility of the sol−gel process for preparing organic−inorganic "molecular composites." Sol−gel-derived polymer composites incorporating an inorganic component, instead of a purely organic system, generally have enhanced modulus, transparency, surface hardness, and heat resistance.[25] Polyaniline/silica and polyimide/silica composites have been created,[26,27] for example, with interacting polymer and silica networks. The range of interaction between the organic and inorganic components can vary from no bonding to significant covalent cross-linking between the two networks. For the polyimide/silica system,[27] the hybrid composite films were created through the hydrolysis and polycondensation of (3-aminopropyl)triethoxysilane (both in monomer form and within the polymer backbone) and TEOS in an *N*,*N*-dimethylacetamide (DMAc) solution of polyamic acid. Silica was incorporated within the polyamic acid in order to create covalent bonding between the polymer and silica network during the sol−gel process. After allowing the hydrolysis reaction to proceed for approximately 6 h, the resulting homogeneous mixture was cast onto a glass plate. The polyimide/silica hybrid film resulted after progressively curing the film at 60, 200, and 300 °C. In comparison with pure polyimide, films containing the cross-linked silica network yielded higher ultimate strength, higher initial Young's modulus, but lower ultimate elongation.[27]

ORMOCERs doped with dyes have been examined because of their potentially superior mechanical and optical properties for use in integrated optics applications.[28,29] Isolating active organic species in a rigid matrix inhibits intermolecular interaction and intramolecular rearrangement, and also potentially protects the active molecule from environmental attack. Examples of films emitting in the visible, as well as the infrared spectral region, have been reported.[28] The inorganic

framework in these films may be based on ZrO_2 or TiO_2, rather than SiO_2. The ZrO_2 matrix is noted for having a high refractive index and good chemical resistance and can be created by mixing zirconium(IV) propoxide, 3-glycidyloxypropyltrimethoxysilane (GLYMO; organic modifier), and a solvent mixture of ethanol and acetic acid.[28] Sol−gel-derived organic−inorganic hybrid films have also been introduced as emissive layers in light emitting devices (LEDs).[30] The resulting dye-containing sol−gel glass layer may exhibit high thermal stability, good transparency, and the ability to reduce the translational, rotational, and vibrational degrees of freedom of the trapped dye molecule.

Second-order nonlinear optical properties of dye-containing hybrid films, created using the sol−gel approach in conjunction with poling, have been another area of active interest because of potential application in optical switching, optical waveguides, and signal processing.[31,32] A photopatternable transparent ORMOCER, with low transmission losses in the near-IR range (0.2 dB/cm at 1310 nm and 0.3 dB/cm at 1550 nm), has been created via the sol−gel processing of functionalized pentafluorophenylalkoxysilanes followed by cross-linking reactions.[33] The low losses can be attributed to the fluorination of the organic component of the hybrid as well as to reduction in the number of Si−OH groups within the network. In addition to the high transparency, the fluorinated ORMOCERs show a number of other desirable properties for use in waveguide applications, including good wetting and adhesion on various substrates (e.g., glass, silicon, and several polymers), low processing temperatures (post bake below 160 °C), high thermal stability (decomposition >250 °C), and tunable refractive index. A high gain (maximum net gain of 54 dB/cm) active planar waveguide, based on an organic−inorganic hybrid glass film doped with a laser dye (e.g., Rhodamine B), has also been reported.[34] The high gain of the active waveguides renders them suitable for solid-state lasers.[35] Note that conventional methods of glass waveguide preparation do not readily allow for the incorporation of organic molecules because of the high temperatures involved.

Although sol−gel processed hybrid films result from chemical condensation reactions and are typically amorphous (at least before annealing), modification of the sol−gel process to include structure-directing surfactant molecules can lead to self-assembly of partially ordered phases.[36,37] The film structure formation can be controlled through the silica-to-surfactant ratio as a result of charge matching at the interface. A silica mesostructured film containing the dye-bound surfactant 11-ferrocenylundecylammonium bromide, for example, has been obtained (Figure 1) by spin-coating of the hybrid sol.[37] First, TEOS is partially hydrolyzed by a stoichiometric amount of water mixed with ethanol under acidic conditions. As the solution becomes homogeneous during the hydrolysis step, a surfactant solution of the 11-ferrocenylundecylammonium bromide salt is added, and the resulting solution is mixed at room temperature for approximately 1 h. Spin-coating the hybrid sol onto a substrate and vacuum curing for 1 h at 100 °C leads to the desired product. An X-ray diffraction pattern of the hybrid film indicates that it has a lamellar structure with a (100) *d* spacing of 36.3 Å, which is approximately twice as long as the 11-ferrocenylundecylammonium surfactant molecule. Related films prepared using a similar modified sol−gel method mimic the structure of seashell and might be suitable for applications such as automotive finishes, hard coats, and optical hosts.[38]

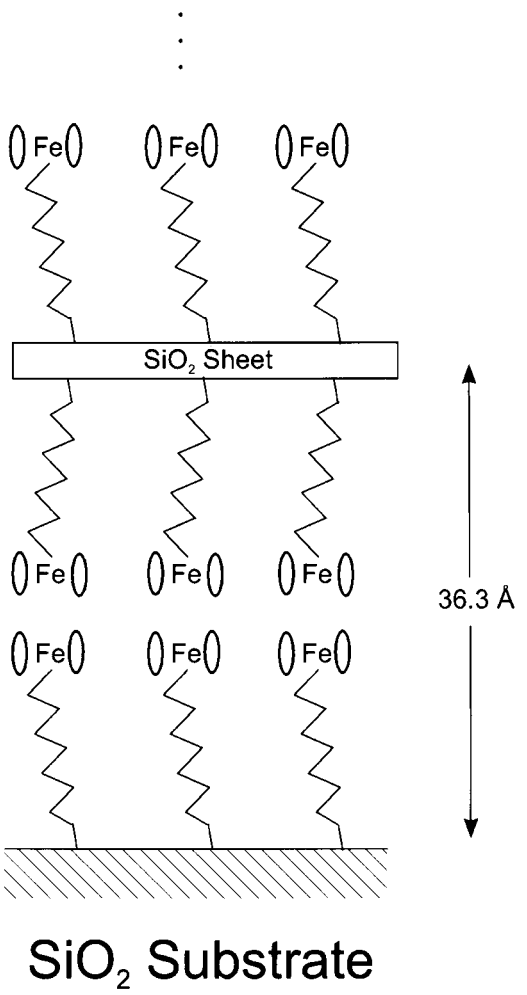

Figure 1. Schematic representation of the local thin-film structure formed by spin coating a sol containing partially hydrolyzed TEOS and the dye-bound surfactant, 11-ferrocenylundecylammonium.[37] The 36.3 Å lattice spacing was determined from X-ray diffraction.

Although the silica networks described above generally form in a somewhat random fashion through a condensation reaction and are nominally insoluble, other hybrids are readily soluble in common organic and aqueous solvents and will crystallize from solution upon evaporation of the solvent. The organic−inorganic perovskites and related systems provide an extensive array of examples of this type of system.[5] Both the metal halide component and the organic cations are soluble in polar solvents such as alcohols, acetonitrile, ethylene glycol, water, hydrochloric acid, hydrobromic acid, hydriodic acid, or acetic acid. The wide range of chemical interactions (ranging from covalent bonding within the metal halide framework to hydrogen bonding and van der Waals interactions within the organic layer) drive the components to assemble into the desired crystal structure under a wide range of conditions, thereby rendering these materials very amenable to solution processing techniques.

Spin coating is one method of depositing thin films of the soluble self-assembling organic−inorganic compos-

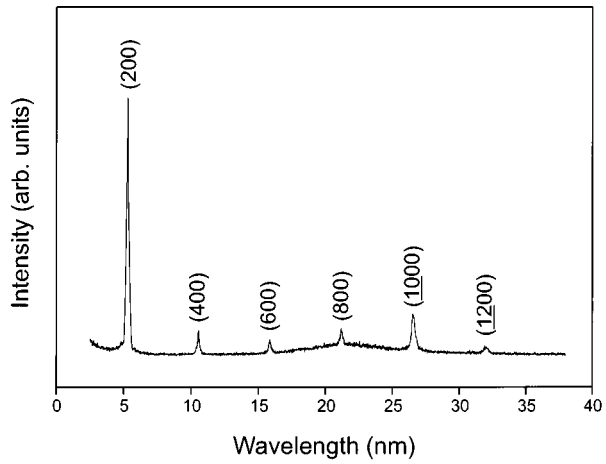

Figure 2. Room-temperature X-ray diffraction pattern for a spin-coated film of $(3\text{-FPEA})_2SnI_4$, where 3-FPEA = 3-fluorophenethylammonium.[17] The film was spun at 3000 rpm onto a quartz disk, from a solution containing 20 mg of the hybrid dissolved in 1.6 mL of methanol. The indices of the X-ray peaks are shown in parentheses, indicating the high degree of crystallinity and preferred orientation for the film.

ites on a variety of substrates including glass, quartz, sapphire, and silicon.[5,39−41] The process involves finding a suitable solvent for the hybrid, preparing a solution with the desired concentration, and applying drops of the solution to a spinning substrate. As the solution spreads on the substrate, it dries and leaves a deposit (generally crystalline) of the hybrid. Figure 2 shows a typical X-ray pattern for a spin-coated film of an organic−inorganic perovskite.[17] Notice that only (2*h* 0 0) reflections appear in the pattern, indicating that the films are highly crystalline and oriented, with the plane of the perovskite sheets parallel to the substrate surface. The relevant parameters for the deposition include the choice of substrate, the solvent, the concentration of the hybrid in the solvent, the substrate temperature, and the spin speed. Pretreating the substrate surface with an appropriate adhesion promoter may improve the wetting properties of the solution. After deposition, low-temperature annealing (T < 200 °C) of the films is also sometimes employed to improve crystallinity and phase purity. Spin processed hybrid films are generally very smooth (mean roughness ∼1−2 nm),[42] enabling their use in device structures including, for example, LEDs and TFTs.[12,15−17] Air and moisture sensitivity of the perovskite films has been addressed by incorporating the nanocrystalline hybrids [e.g., $(C_6H_5C_2H_4NH_3)_2PbI_4$] within a transparent poly(methyl methacrylate) (PMMA) matrix using a spin-coating process.[43] As an example of a nonperovskite hybrid, sequential spin-coating of polysaccharides and $CaCO_3$ in the presence of an acid polymer has also been used to prepare layered polymer/calcium carbonate multilayer films.[44]

In addition to spin coating, other solution techniques for depositing the organic−inorganic hybrids include ink-jet printing, stamping, and spray coating, thereby opening up the possibility of depositing these materials under a wide range of conditions and on many different types of substrates (including flexible plastic). All of these techniques require a suitable solvent for the organic−inorganic hybrid.

III. Intercalation Reactions

In some cases, a suitable solvent cannot be found for a self-assembling organic−inorganic hybrid. This may arise when the organic and inorganic components of the structure have incompatible solubility requirements or when a good solvent for the hybrid does not wet the substrate surface. Recently, a dip-processing technique[42] has been described (Figure 3) in which a predeposited (vacuum evaporation or solution deposited) metal halide film is dipped into a solution containing the organic cation. The solvent for the dipping solution is selected so that the organic salt is soluble, but the starting metal halide and the final organic−inorganic hybrid are not soluble. In the case of the organic−inorganic perovskites and related hybrids for which there is a large driving force toward the formation of the hybrid structure relative to the organic and inorganic components, the organic cations in solution intercalate into and rapidly react with the metal halide on the substrate and form a crystalline film of the desired hybrid.

For the perovskite family, $(R{-}NH_3)_2(CH_3NH_3)_{n-1}M_nI_{3n+1}$ (R = butyl or phenethyl; M = Pb or Sn; n = 1 or 2), toluene/2-propanol mixtures work well as the solvent for the organic salt and the dipping times are relatively short (several seconds to several minutes, depending on the system).[42] A film of $(C_4H_9NH_3)_2PbI_4$, for example, was formed from a vacuum deposited film of PbI_2 (Figure 3a) by dipping it into a butylammonium iodide solution. The dipping time for the reaction was 1−3 min, depending on the thickness of the lead(II) iodide film (2000−3000 Å). After dipping, the films were immediately immersed in a rinse solution of the same solvent ratio as the initial dipping solution (but with no organic salt) and dried in a vacuum. As seen in Figure 3b, the resulting films exhibit the characteristic (00*l*) reflections for the organic−inorganic perovskite (and sometimes weak off-axis reflections), as well as the characteristic photoluminescence spectrum (Figure 3c).

The three-dimensional perovskite $CH_3NH_3PbI_3$ has also been made using a similar two-step dipping technique. However, in this case, the required dipping times are longer (1−3 h). Presumably, the longer dipping times are required as a result of the absence of a van der Waals gap in the three-dimensional structure. In $(C_4H_9NH_3)_2PbI_4$ and related layered systems, butylammonium cations can readily diffuse to the boundary with the unreacted PbI_2 through the van der Waals gap within the organic bilayer of the reacted material at the film surface. In the three-dimensional compound, this pathway is not operative, and therefore, the reaction proceeds at a much slower rate. Note that layered perovskites with diammonium cations (which also lack a van der Waals gap) similarly require a longer period for the reaction to complete.

Although the dipping technique has been demonstrated with the hybrid perovskites,[42] it should also be relevant for other organic−inorganic hybrids. The primary requirements for this process include a strong thermodynamic driving force for the formation of the hybrid and a means for the organic species to diffuse through the resulting hybrid so that it can progressively interact with the unreacted inorganic material below the already reacted surface layer of the film. This

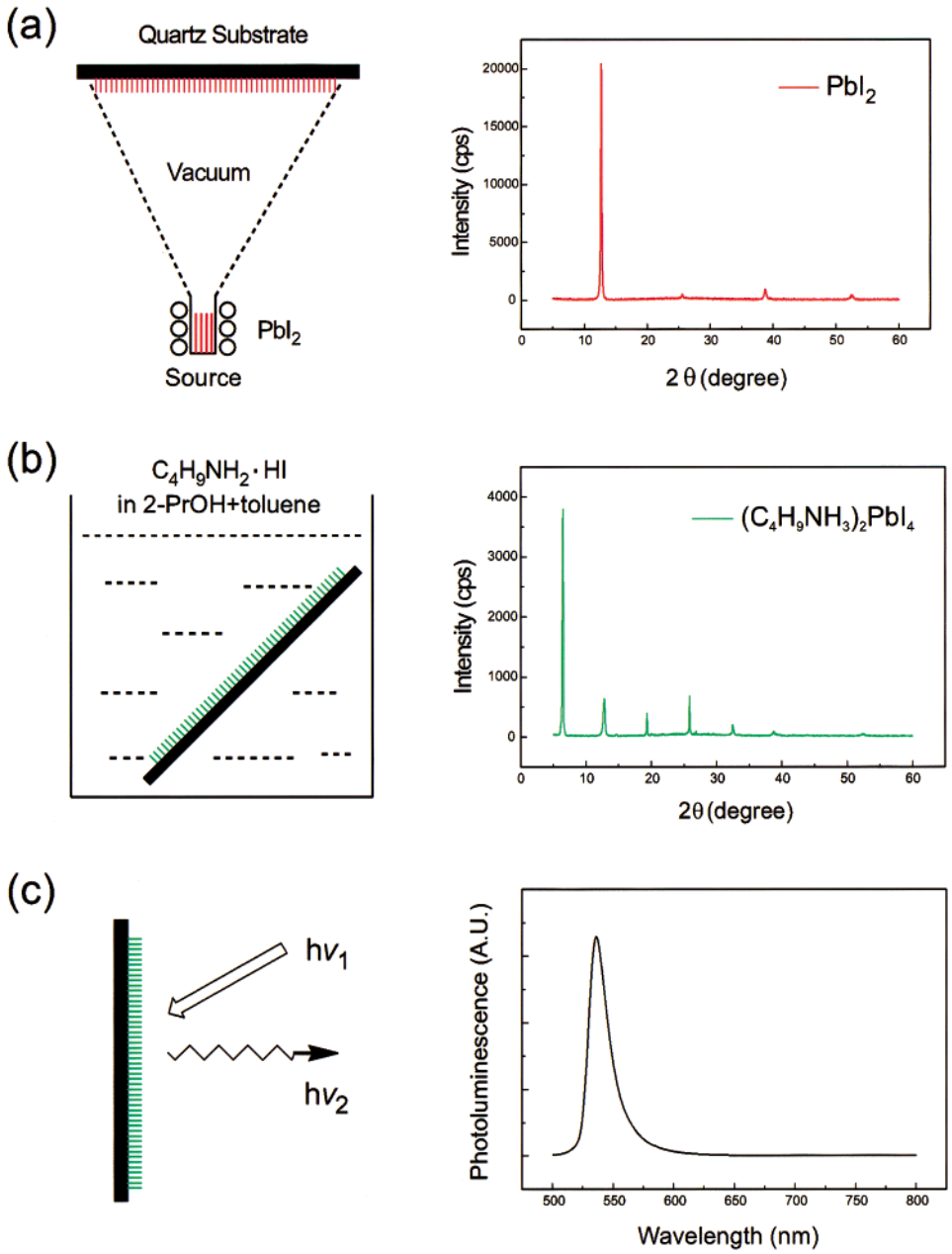

Figure 3. Schematic representation of the two-step dipping technique.[42] In (a), a film of the metal halide (in this case PbI_2) is deposited onto a substrate using vacuum evaporation, yielding an ordered film with the characteristic X-ray pattern. The metal halide film is then (b) dipped into a solution containing the organic cation (in this case $C_4H_9NH_3^+$). The solvent (e.g., a mixture of 2-propanol and toluene) should be a good solvent for the organic cation but not for the metal halide or the resulting hybrid. The resulting film after dipping has the characteristic X-ray pattern for the hybrid perovskite, as well as (c) the characteristic room-temperature photoluminescence spectrum.

technique eliminates the need for a simultaneously suitable solvent for the organic and inorganic components of the structure (as would be required for solvent techniques) or the need to heat the organic component (as would be required for thermal evaporation techniques). Furthermore, mixed organic cation hybrid films can be created by dipping the inorganic film into a solution containing multiple organic cations. For applications that require patterning, the dipping technique may also provide a promising pathway, since prior to the dipping step the surface of the film can be coated with a resist so that only selected areas will be exposed to the organic cation in solution. It should be noted, however, that during the reaction of the organic cation with the inorganic film there is often substantial grain growth, potentially leading to morphologically rough films.

An analogous version of the two-step dipping process involves subjecting a metal halide film (predeposited by vacuum deposition) to a vapor of the organic salt.[45] Lead(II) bromide films, for example, can be exposed to alkylammonium bromide, vaporized by heating at a base pressure of 10^{-5} Torr. As for the two-step dipping technique, wherein an organic salt in solution can react with a metal halide film, in this case, essentially the same process happens with the organic salt in a vapor phase. As for the solution-based process, the reaction presumably proceeds through the intercalation of the organic cation into the van der Waals gap of the initial metal halide film. After the organic molecule enters the

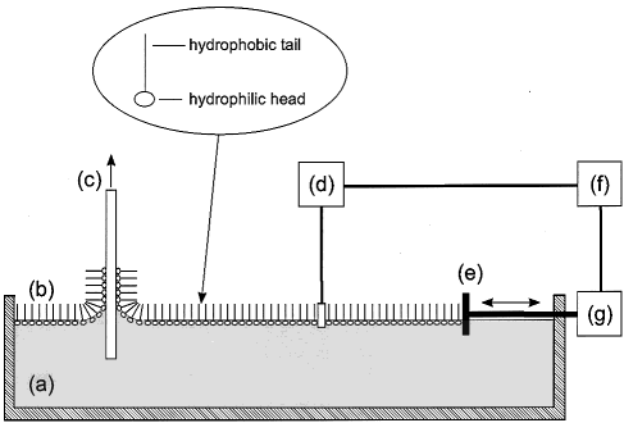

Figure 4. Schematic representation of a Langmuir−Blodgett setup consisting of (a) a bath containing (b) the monolayer of amphiphilic molecules at the gas-fluid interface, (c) the substrate being withdrawn from the bath, and (d) a balance that measures the surface pressure of the monolayer, which is being generated using the moveable barrier (e). The moving barrier is controlled using a feedback device (f), which gets the information from the pressure sensor and adjusts the barrier position using the motor (g).

structure, it then reacts with the metal halide framework by a solid-state reaction between the metal halide and the intercalated alkylammonium bromide molecule. Both the solution-based and vapor-phase techniques demonstrate the strong driving force favoring the formation of the perovskite hybrids.

IV. Layer-by-Layer Assembly

The ability to assemble hybrid films a monolayer at a time allows for layer-by-layer control of thickness, composition, and physical properties. Such control provides an important path for the creation of new hybrid materials for organic−inorganic electronic devices and/or molecular electronics. Several solution-based approaches are currently available for controlling growth with monolayer precision.

Langmuir−Blodgett (LB). One of the earliest methods of layer-by-layer assembly is the classical LB technique (Figure 4),[46,47] which was developed over 65 years ago. Molecules, usually amphiphiles, are first compressed to a close-packed monolayer at a liquid (subphase)−gas surface using a moveable barrier and then mechanically transferred as a monolayer assembly to a solid support that is passed through the surface. The pressure applied by the moveable barrier in the Langmuir trough enables the amphiphilic molecules at the liquid−gas interface to get close enough together for the relatively weak van der Waals interactions between the molecules to become important and to achieve a nominally close-packed monolayer. The most common interface at which to create the Langmuir monolayer is the air−water surface. Multilayer films are formed through repeated deposition cycles.

One approach to forming hybrid LB multilayers is to base the targeted structures on known bulk solids. The metal phosphonates provide a range of interesting layered compounds, containing sheets of metal ions that are bonded above and below by layers of organophosphonates.[48] The phosphonate ligands bridge the metal ions within a metal layer, thereby creating an extended inorganic lattice. Metal octadecylphosphonate films have been formed, for example, with a number of cations, including Ca^{2+}, Cd^{2+}, Mg^{2+}, and Mn^{2+}.[49] The films are prepared by spreading octadecylphosphoric acid onto the surface of an aqueous bath containing a salt of the appropriate metal. The pH of the solution is adjusted to an appropriate level (5.2−8.1, depending on the metal ion) with HCl or KOH. Because the metal phosphonates are soluble in acid solutions, the metal ions are not incorporated into the Langmuir monolayer if the solution pH is too low. Likewise, if the pH of the solution is too high, the monolayer becomes too rigid to transfer because of phosphonate cross-linking of the metal ions. Therefore, the optimum pH for obtaining LB films with an extended inorganic lattice is the highest possible pH at which the monolayer is not too rigid to transfer.[49]

The metal octadecylphosphonate LB films are transferred onto a substrate by compressing the Langmuir monolayer to an optimum pressure using a moveable barrier and then slowly lowering a hydrophobic substrate through the film, transferring a monolayer in a tail-to-tail fashion. The substrate is then similarly raised from the solution, leaving a head-to-head bilayer. The Mn^{2+}-, Cd^{2+}-, and Mg^{2+}-based LB films adopt $M(O_3PR)\cdot H_2O$ type structures, whereas the Ca^{2+} analogues form in a 1:2 metal-to-organic ratio, $Ca(HO_3PR)_2$. The different structures demonstrate the important role that the inorganic lattice plays in organizing the LB films.[49] The hybrid Mn^{2+} multilayer structure also undergoes a magnetic ordering transition at 13.5 K, resulting in a canted antiferromagnet and demonstrating that magnetic ordering phenomena can be incorporated into LB films.[49] LB films based on mixed-valent cyanometalates intercalated between bilayers of dimethyldioctadecylammonium cations also exhibit a ferromagnetic transition at low temperature.[50] The magnetic LB multilayer structures are particularly interesting because changing the length of the alkylphosphonate component can regulate the distance between magnetic layers.

The metal phosphonate bonding can be tuned among known bonding motifs by changing the metal ion, thereby providing some degree of control over the packing of the organic molecules. In addition to the divalent metal-based systems, similar LB films have been prepared using octadecylphosphonic acid and azobenzene-derivatized phosphonic acid with various divalent, trivalent, and tetravalent metal ions (e.g., Zr^{4+}, La^{3+}, Gd^{3+}, and Ba^{2+}).[51−53] The resulting thin film structures are generally the same as the corresponding solid-state structures. The azobenzene-derivatized phosphonic acids, 4-(4′-(3″-pentyloxy)phenyl)azophenylbutylphosphonic acid and 4-(4′-propoxyphenyl)azophenylbutylphosphonic acid, undergo rapid and reversible trans to cis photoisomerization within a zirconium phosphonate LB film.[53] Note that these latter films are deposited using a combination of the LB technique and self-assembly (see below), allowing for non-LB-active molecules to be deposited in the multilayers and therefore enabling structural modification of the azobenzene molecules to deter aggregation and enhance photoisomerization.

Organic−inorganic perovskites, based on a metal halide framework, have recently been formed using the

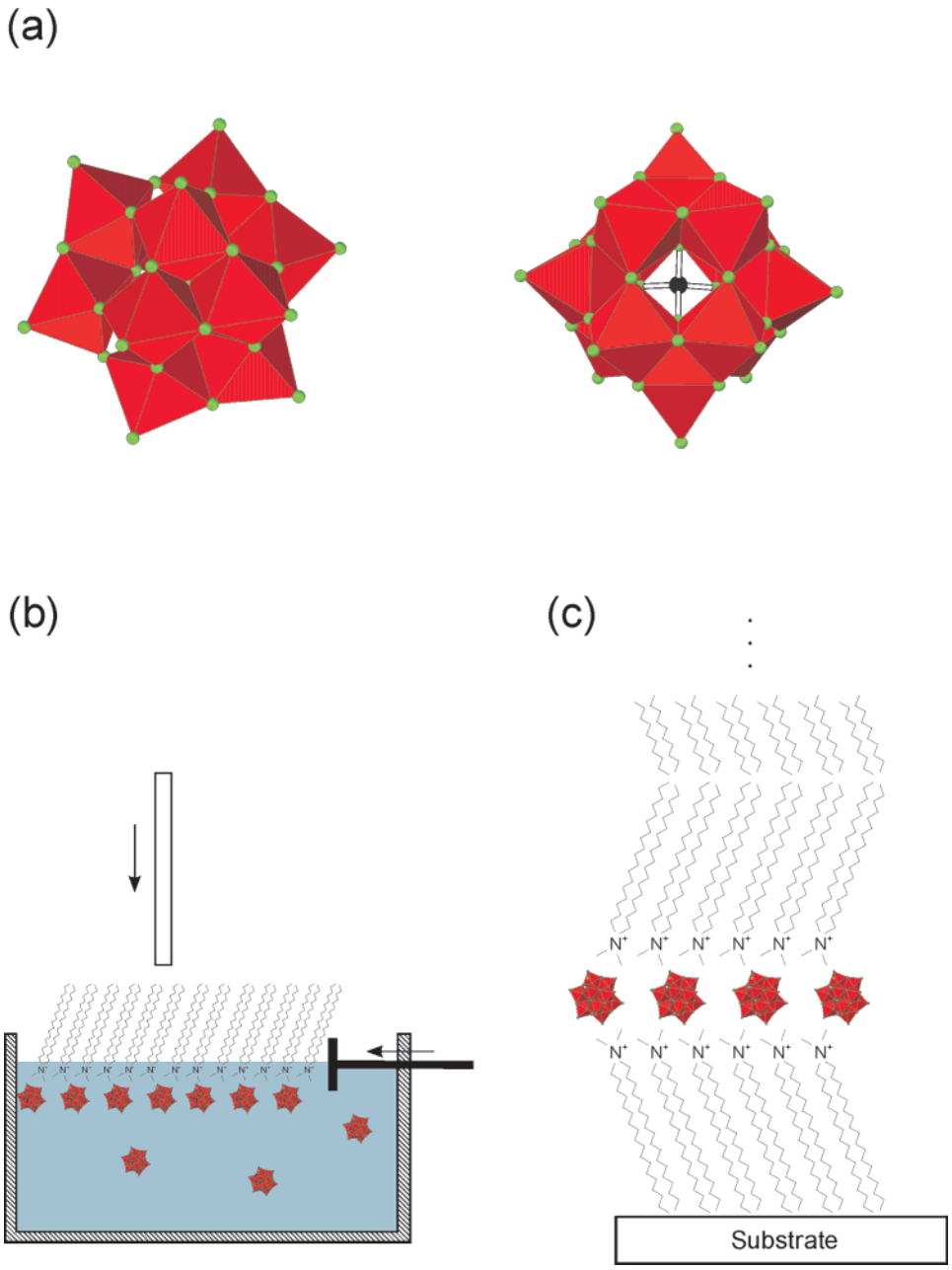

Figure 5. (a) Two views of the Keggin polyanion, $[X^{n+}M_{12}O_{40}]^{(8-n)-}$. The MO_6 octahedra are represented in polyhedral form, with the oxygen atoms at the apexes. In the orientation depicted in the right panel, the tetrahedral coordination of the X atom is apparent. (b) Langmuir monolayer of dioctadecylammonium cations and adsorbed Keggin polyanions. (c) The resulting LB film formed by repeated dipping of the substrate through the Langmuir monolayer.

LB technique.[54] A monolayer of docosylammonium bromide ($C_{22}H_{45}NH_3Br$) is spread on a subphase containing lead(II) bromide and methylammonium bromide. After compressing the monolayer to 30 mN m^{-1}, vertical dipping is used to transfer the monolayer to a fused quartz substrate, which has been made hydrophobic by treatment with hexamethyldisilazane. Only the single layer perovskite structure is formed in this process (i.e., one in which a single lead(II) bromide sheet alternates with a bilayer of organic cations), indicating that methylammonium cations are, for the most part, not incorporated into the structure.

Polyoxometalate anions have also been incorporated into hybrid LB films.[55] Perhaps the best known of these clusters are the Keggin polyanions (Figure 5a),[56] $[X^{n+}M_{12}O_{40}]^{(8-n)-}$, which consist of a central heteroatom (e.g., X = P, Si, Co, Fe, B, Cu, Ge, or As) in a tetrahedral cavity, surrounded by four M_3O_{13} groups (M = W or Mo, i.e., three edge-sharing octahedra). A useful property of these clusters is their solubility and stability in aqueous and nonaqueous solvents. In addition, the ability to accept various numbers of electrons (providing the possibility of mixed valency) makes the anions noteworthy components with which to impart interesting electronic, magnetic, and optical properties to the hybrids. They have been used, for example, as magnetic entities in conducting hybrid radical salts.[57] For LB deposition, a Langmuir monolayer (Figure 5b) of positively charged dimethyldioctadecylammonium cations is used to template the adsorption of the Keggin polyanions. The resulting LB films (Figure 5c) provide substantial flexibility in terms of incorporating the properties of the polyoxometalate clusters within a hybrid multilayer.

Scheme 2

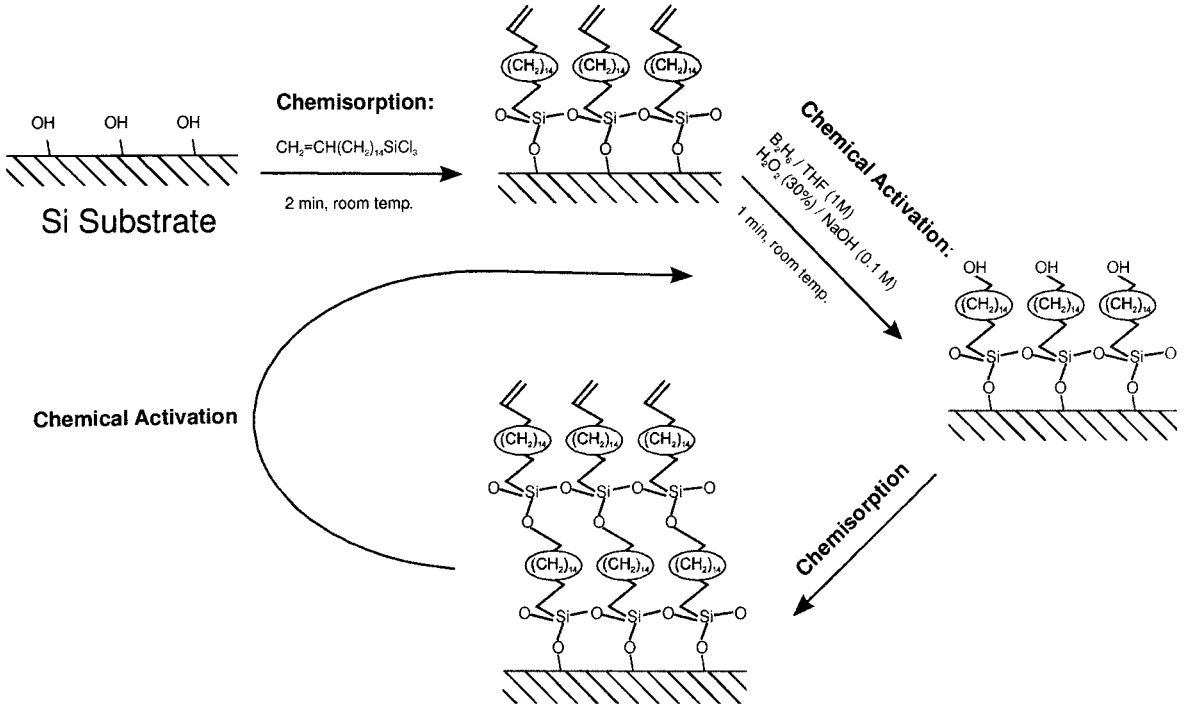

Finally, a smectite (clay)−amphiphilic ruthenium(II) complex hybrid LB film has been demonstrated.[58] A chloroform solution of the ruthenium(II) complex, [Ru(1,10-phenanthroline)$_2$(4,4′-dioctadecyl-2,2′-bipyridyl)]$^{2+}$, is first spread onto an aqueous subphase containing either an exfoliated saponite or hectorite suspension. The Ru(II) complex molecules form a self-assembled monolayer on the water surface, with clay particles adsorbed underneath. A composite film of the Ru(II) complex and clay particles can therefore be formed on a hydrophilic glass plate using the vertical dipping method. Incorporation of the clay layer may enhance the mechanical strength of the film and also help to order the adsorbed organic molecules into a two-dimensional array. Similar hybrid films consisting of exfoliated anionic MoS_2 sheets and dihexadecyldimethylammonium cations have also been prepared.[59]

Self-Assembly. Whereas the LB technique requires a preformed monolayer at the surface of a liquid, self-assembled monolayers form spontaneously upon immersion of the substrate into a uniform solution.[60] In the case of self-assembled monolayers and multilayers, chemisorption provides the driving force that enables the molecules to be pushed close together on a surface (replacing the moveable barrier in the LB technique). Chemisorption leads to covalent or ionic bonding of the "head" group of the molecule to a specific site on the surface. The technique is particularly attractive because of its simplicity and because substrates of arbitrary shape can be coated.

Although self-assembled monolayers and multilayers of organic molecules have been extensively studied,[60] multilayered hybrid films have also been created by, for example, a sequential adsorption and chemical activation process (Scheme 2).[61] A bifunctional surfactant is employed, which has both the usual polar "head" as well as an apolar terminal group that can be converted into a suitable polar group after completion of the adsorption step. The technique was originally demonstrated using HTS (15-hexadecenyltrichlorosilane).[61] The $SiCl_3$ function enables a covalent attachment to surfaces rich in hydroxyl groups, whereas the ethylenic double bond provides a convenient path for the activation of the monolayer via hydroboration and hydrogen peroxide oxidation to terminal hydroxyls. The new terminal hydroxyls can then react with a new layer of surfactant trichlorosilanes, leading to an alternating sequence of silicon oxide and surfactant layers. The initial process failed to yield multilayer structures more than two to three layers thick, presumably because of imperfect ordering of alkyl chains within the layers and incomplete surface reaction. More recently, thicker and better-ordered multilayer films were created using a modification of the original process in which interlayer bonds are formed starting from carboxylates rather than ethylenic double bonds.[62] An analogous silane-based self-assembly process has also been described for the creation of nonlinear optical materials.[63]

Another important modification of the self-assembly technique involves the sequential adsorption of the components of thermodynamically stable and insoluble layered metal phosphonates, such as zirconium 1,10-decanebisphosphonate, $Zr(O_3PC_{10}H_{20}PO_3)$.[64] The process (Scheme 3) involves first exposing a Si substrate to a warm (50 °C) aqueous solution of a silanol, producing a monolayer of covalently anchored phosphonate groups. After rinsing with water, the surface is exposed to an aqueous $ZrOCl_2$ solution, followed by another rinse, and exposure to an aqueous 1,10-decanebisphosphonic acid solution. Repetition of the second and third steps leads to the hybrid multilayer film. The process also works for other metal phosphonates, using alternating immersions in appropriate metal salt and bis(phosphonic acid) solutions, and films containing over 100 layers can now be grown routinely.[65] In contrast to the silane-based process (Scheme 2), no separate chemical activation step

Scheme 3

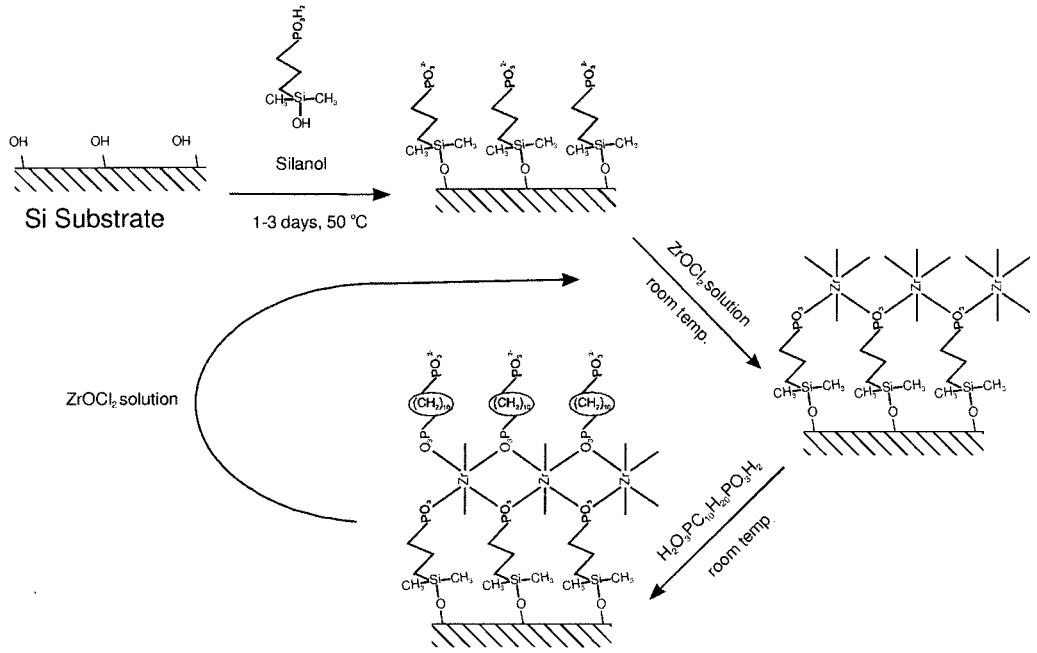

is required for this procedure. This simplifies the process and eliminates the need to expose the film to the harsh conditions that are typically required to activate the surface functional groups.

The ~24 Å cross-sectional area provided by the zirconium bisphosphonate framework for each organic molecule enables substantial flexibility with respect to the types of functional groups that can be accommodated in the bisphosphonate molecule.[65,66] Multilayer structures consisting of polar dye monolayers [e.g., 4-{4-[*N*,*N*-bis(2-hydroxyethyl)amino]phenylazo}phenylphosphonic acid; Scheme 4] alternating with and joined by

Scheme 4

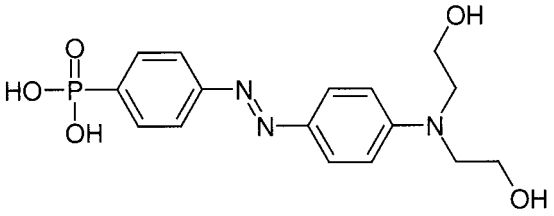

relatively immobile Zr phosphate−phosphonate interlayers have, for example, been created using a similar process to that described above for the zirconium 1,10-decanebisphosphonate system.[67] The dye molecules have a phosphonate group at one end and a hydroxyl at the other. The phosphonate end of the molecule preferentially adsorbs on a Zr^{4+} layer, with the exposed hydroxyl group being later converted to an organic phosphate with $POCl_3$. Adsorbing another Zr^{4+} layer on top of the phosphate layer completes the cycle. The substantial second harmonic generation (SHG) in these films (similar to that observed in $LiNbO_3$) shows that the multilayers have polar order and that this ordering does not decrease with increasing numbers of alternating layers. The relatively rigid inorganic layers of the hybrid impart both orientational and thermal stability to the hybrid. In the example given, SHG intensity did not diminish after annealing for 3 h at 150 °C in air. Orientational randomization occurs at much lower temperature in most traditional LB films and poled polymers.[67]

Nonlinear optical properties have also been designed into analogous hybrid films based on hafnium(IV) bisphosphonate.[68,69] The multilayers are created by alternately dipping an appropriately functionalized silicon oxide substrate into aqueous solutions of $HfOCl_2$ and a bis(phosphonic acid). A π system (e.g., phenyl or stilbyl group) is incorporated between an electron donor and acceptor within the bisphosphonate molecule. A typical example is aryl-(4-diethylphosphonate)-10-decylphosphonic acid ether (Scheme 5). The orientation of the

Scheme 5

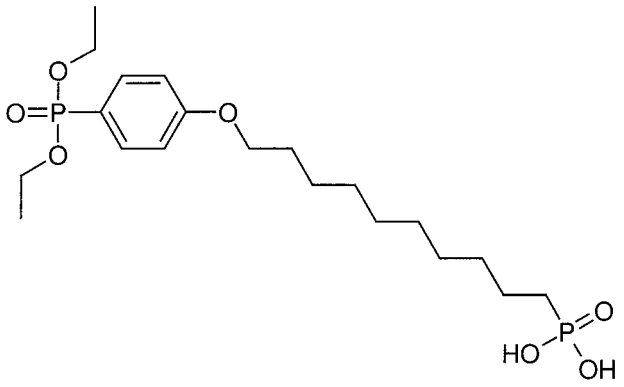

molecule is maintained by functionalizing one end of the bisphosphonate with a phosphonic acid group, while leaving the other end "protected" in phosphonate ester form. This ensures oriented binding of the molecule to Hf on the surface through the acid end. After adsorption of the bisphosphonate molecule, the phosphonate ester must be deprotected (hydrolyzed) using a relatively dilute (0.5 M) HCl solution at near-ambient temperatures (40−80 °C), before the next immersion step in the $HfOCl_2$ solution.

Of particular interest among the metal phosphonate multilayer structures are examples in which different organic cations are incorporated on distinct layers of the structure. Systems have been demonstrated, for example, in which the different layers consist of electron donor and acceptor molecules, separated by the inorganic metal phosphonate layers.[70,71] In one case, alternating viologen-based acceptor layers and *p*-phenylenediamine donor layers, led to efficient photoinduced charge separation and directional electron transport.[71] Analogous hybrid structures have also been created with a 5,10,15,20-tetrakis(4-phosphonophenyl)porphyrin donor and *N*,*N*′-bis(3-phosphonopropyl)-4,4′-bipyridinium acceptor.[70] Again, evidence was reported for vectorial electron transfer from the donor to acceptor, across the metal (Zr) phosphonate barrier.

In addition to the silanes and metal phosphonates, other building blocks for self-assembled hybrid films have also been examined. In one example, cobalt-diisocyanobenzene and cobalt-1,6-diisocyanohexane multilayers have been assembled on an amine-functionalized silicon surface by repeated sequential immersion in cobalt(II) chloride and 1,4-diisocyanobenzene (or 1,6-diisocyanohexane).[72] The assembly in these structures is based on the strong coordination of the isocyanide ligand to a metal center. Isocyanides bind to a wide range of metal centers because of the ability of the ligand to form stable sigma bonds with high valent metal centers and to accept electrons into vacant π^* orbitals to form π bonds with low-valent metal centers.[72,73] As with the zirconium phosphonate systems, no chemical activation or deprotection is required in order to build up the multilayer structure. XPS and IR studies indicate that the chemistry may be complicated by the partial oligomerization of the isocyanides within the films.[72] Other self-assembled structures based on coordinate covalent bonds include lamellar multilayers analogous to the Hoffmann-clathrates, based on planar metal-cyanide-metal sheets bridged by nitrogen containing ligands (e.g., 4,4′-bipyridine and 1,12-diaminododecane).[74,75] A polymer/inorganic nanoparticle composite film has also been reported, on the basis of the coordinate bonds of pyridine-based polymers and CdS nanoparticles.[76]

Electrostatic Assembly. The LB deposition approach primarily relies upon relatively weak van der Waals forces, leading to marginal mechanical stability of the resulting films. In addition, the process is generally limited to surfactant-like molecules. Layer-by-layer self-assembly relies on stronger covalent or ionic bonding, leading to better thermal and mechanical stability. However, the formation of each layer in the hybrid multilayer structure relies on the chemisorption of individual molecules to the underlying surface. A nearly constant number of active sites must be maintained from layer to layer (i.e., the reaction must proceed to nearly 100% yield in each layer). Defects in one layer will propagate and grow in each successive layer, making it difficult to obtain a large sequence of well-formed layers. An alternative approach, based on the sequential adsorption of polyanions and polycations (Figure 6), relies on electrostatic interaction between oppositely charged layers and can be readily generalized to include polymeric, nanoparticle, clay-like, and colloidal polyions. Because charged species repel each other, each adsorption step is nominally self-limited to the formation of a single monolayer. In addition, the reduced steric demands of the electrostatic interaction (relative to covalent bonding) provide more flexibility in the application of this process, and this factor, along with the large dimensions of the polyion components, also enables the "self-healing" of defects in an underlying layer.

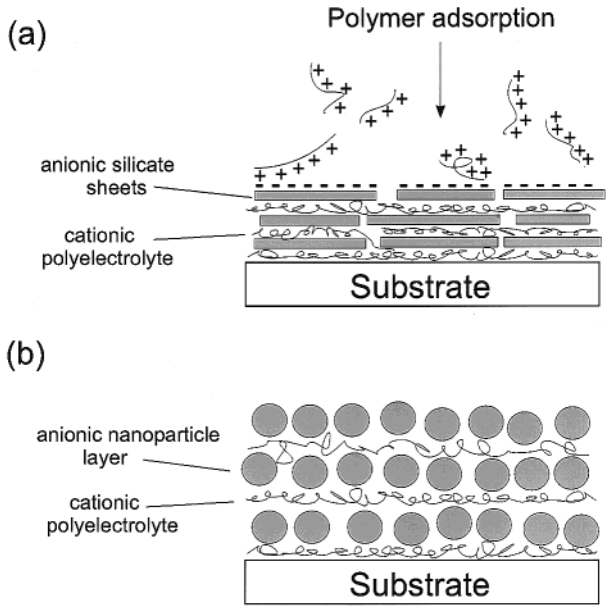

Figure 6. Hybrid multilayer structures formed using electrostatic assembly. In (a), layers of the cationic polyelectrolyte, poly(diallyldimethylammonium chloride), alternate with layers of exfoliated silicate anionic sheets. A new polymer layer is in the process of being adsorbed. In (b), a similar structure is formed but with the clay-like sheets, replaced with negatively charged nanoparticles (e.g., CdSe or CdS).

Early work on layer-by-layer assembly of cationic and anionic colloidal particles[77] has rapidly been extended to include a number of interesting hybrid systems. One approach (Figure 6a) involves the sequential adsorption of the cationic polyelectrolyte, poly(diallyldimethylammonium chloride) (PDDA), and anionic sheets (~1 nm thick) of the layered silicate, Laponite RD (synthetic hectorite).[78] A silicon wafer is first cleaned to provide a hydroxylated surface. An aqueous solution of PDDA is then dripped onto the substrate. The PDDA solution is rinsed off after ~5 s and blown dry with nitrogen. Subsequently, an aqueous dispersion of exfoliated hectorite is dripped onto the surface and rinsed off/blown dry after ~5 s. Repetition of this two-step process provides multilayer films thicker than 0.2 μm in less than 2 h. The process is governed by a balance between adsorption and desorption equilibria of species with appropriate hydrophobicities and charge densities. Note that the large lateral extent of the hectorite sheets (25−35 nm) essentially prevents interpenetration of the polymer and also allows each hectorite layer to cover any packing defects from the underlying layer, thereby providing a mechanism for "self-healing" in the formation of the hybrid multilayers.[78,79] Similar results to those described above for PDDA/hectorite hybrids have also been achieved for PDDA/montmorillonite multilayers deposited on a variety of substrates, including glass, quartz, metal, and plastic.[80] The effect of an applied

voltage during PDDA deposition on film roughness was also noted in this study, as was the ability of the alternating montmorillonite/PDDA layers to heal etch pits up to 700 nm diameter and 30 nm depth.

Polymer-clay composites are expected to possess a unique set of mechanical, electrical, and gas permeation properties. Both the synthetic hectorite/PDDA and montmorillonite/PDDA films have been studied for their potential application as molecular sensors.[81,82] In the case of the hectorite/PDDA system,[81] the hybrid multilayer structures were found to swell reversibly with changes in relative humidity. Water penetrates to depths greater than 139 nm within seconds and desorbs from the film at similar rates. The resulting changes in film thickness appear as a color change, which can easily be observed with the eye. Mechanisms of gas permeation were also examined in montmorillonite/PDDA films deposited on poly(ethyleneterephthalate) (PET) sheets.[82] The films were found to be flexible and crack-resistant, thereby opening the possibility of designing highly selective ultrathin membranes (i.e., little gas diffusion through cracks). The permeation rate of oxygen was found to decrease 6.6 times for a 200 nm thick hybrid film compared to the PET sheet itself, whereas the permeation rate for aqueous vapors did not change at all.

Graphite oxide−PDDA multilayer structures have also been examined.[83] The graphite oxide structure can be envisioned as graphite sheets, where the majority of double bonds have been oxidized to −OH and −COOH groups. The sheets are strongly hydrophilic and therefore dispersible in water (unlike graphite itself), enabling a similar process for multilayer formation to that described above for the clay−PDDA films. Upon subsequent in situ reduction of the graphite oxide to graphite by chemical and electrochemical methods, the conductivity of the film increases dramatically (by a factor of $\sim 10^3$). The potential benefits of the graphite (or graphite oxide)/PDDA multilayers include the ability to control conductivity and magnetoresistance, as well as the potential for excellent adhesion to a variety of surfaces and mechanical flexibility.

Composites consisting of alternating layers of polyelectrolyte and semiconductor (or insulating) nanoparticles have also been formed (Figure 6b) using a similar electrostatic assembly process. Electrostatically layered hybrid multilayer structures consisting of alternating layers of positively charged (protonated) poly(allylamine) (PA) or PPV and negatively charged CdSe nanoparticles have, for example, been demonstrated on glass, indium tin oxide (ITO), and silicon substrates.[84] When the hybrid multilayers are sandwiched between an ITO anode and an aluminum cathode, with an applied voltage, electroluminescence (EL) is observed. The CdSe/PPV devices yield a broad, nearly white emission, with a much smaller turn-on voltage compared to that of the CdSe/PA devices. The lower operating voltage indicates that PPV acts as a charge transport layer in the CdSe/PPV devices. Note that emission from CdSe particles can be tailored by selecting nanoparticles of different size.[85] In the reported EL devices, the average diameter of the particles was 4.9 nm, with a standard deviation of 1.3 nm. The relatively large particle size distribution leads to a broad photoluminescence spectrum (as for the EL spectrum), which appears nearly white in color. In addition to being able to control the spectral characteristics of the emission by tailoring the inorganic nanoparticles, the polymer component can also be modified to improve the transport properties of electrons and holes (it is the balanced injection of both carriers into the emitting component of the structure that enables efficient emission).

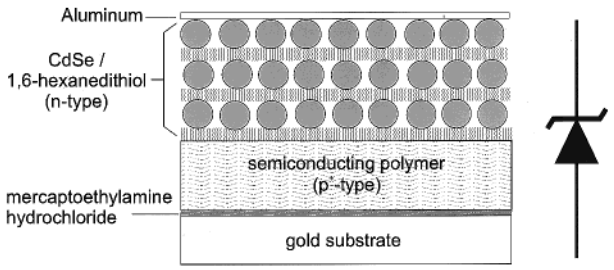

Figure 7. Schematic representation of a p^+-n Zener diode, consisting of a mercaptoethylamine-treated gold anode, a layer of p^+-doped polypyrrole or poly(3-methylthiophene), an n-type multilayer of CdSe and 1,6-hexanedithiol, and an aluminum cathode.[86] The corresponding diagram for a Zener diode is shown alongside the device.

Electrically rectifying devices (Zener diodes) have similarly been prepared using a two-layer configuration (Figure 7), consisting of a p^+-doped semiconducting polymer [polypyrrole or poly(3-methylthiophene)] layer and a n-type multilayer structure of CdSe and 1,6-hexanedithiol.[86] The CdSe particles range from 35 to 37 Å in diameter and are capped with trioctylphosphine oxide. The multilayer structures are created by alternatively dipping the substrate into an aqueous 1,6-hexanedithiol solution for at least 12 h and a CdSe nanoparticle dispersion in butanol for 7−8 h. A pretreated (using mercaptoethylamine hydrochloride) gold surface acts both as the substrate and as the anode, while a layer of aluminum is deposited on top of the device to act as the cathode. By controlling the level of doping in the p-doped polymer, an asymmetrically doped junction can be created, leading to rectifying behavior under forward bias and Zener breakdown in reverse bias.[86]

Other larger band gap nanoparticles based on, for example, PbI_2 or TiO_2, have also been incorporated within an electrostatically self-assembled hybrid multilayer structure.[87,88] In the case of the TiO_2 structures, up to 60 TiO_2 nanoparticle/poly(sodium 4-styrenesulfonate) hybrid layers have been deposited. The optically transparent hybrid films are potentially useful for ultraviolet filters for optics and packaging materials, nonlinear optical components, membranes for nanofiltration, antireflective coatings, n-type semiconductor or dielectric layers, chemical sensors, or coatings to maintain an organic and bacteria-free environment.[88] On the other side of the band gap spectrum, metal nanoparticle/polymer multilayer structures have also been formed.[89] Structures based on magnetic nanoparticles[90] provide one means of controlling the deposition and spacing of magnetic grains of nominally uniform size.

All previously discussed layer-by-layer techniques have primarily focused on achieving ordered multilayers along one dimension, with nominally uniform layers in the other two dimensions. For many applications, the ability to control ordering within the layers is also

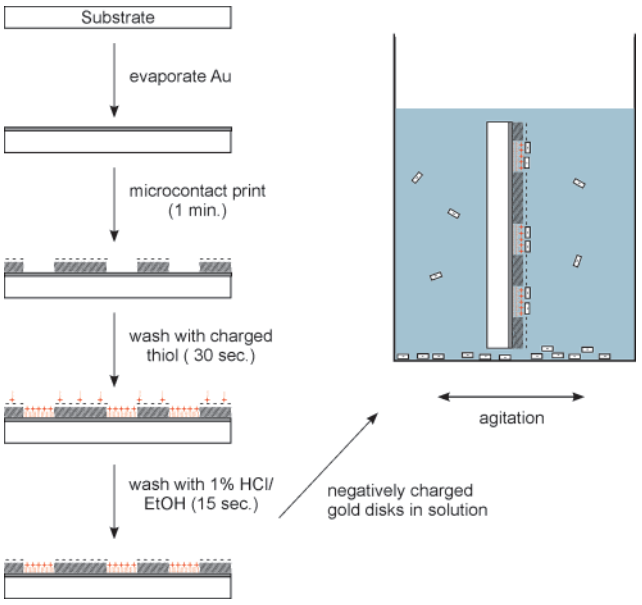

Figure 8. Schematic representation of the electrostatic process used to direct the patterning of charged gold disks on a substrate.[91]

desirable (e.g., to pattern device configurations). Recently, the electrostatic assembly process has been used to direct the patterning of gold disks (~10 μm diameter) on functionalized surfaces (Figure 8).[91] Surfaces with patterned charge can be generated, for example, using microcontact printing, which can be accomplished by stamping a gold film with a poly(dimethylsiloxane) stamp inked with $HS(CH_2)_{15}COOH$, washing with an ethanolic solution of charged thiol, and performing a final wash with 1% HCl/ethanol to remove any electrostatically bound material. Gold disks are made by electrodeposition in a photoresist mold on a silicon surface. After removing the photoresist (with a rinse in acetone) the gold disks can be removed from the silicon surface by sonication in a beaker of charged thiol. The resulting thiol-coated disks can be further coated with an oppositely charged polymer [hexadimethrine bromide for negatively charged gold and sodium poly(vinylsulfonate) for positively charged gold] by immersion in an aqueous solution of the polymer for 10 to 30 min. The patterned substrate can then be placed into a suspension of the gold particles for a few minutes and briefly into a dish of heptane, before being allowed to dry (the heptane reduces capillary forces after removal from the solvent). The charged gold disks are found to deposit as disordered aggregates on regions of the substrate presenting opposite charge.

Note that electrostatic interactions have a longer range than hydrophobic or hydrogen-bonding interactions. Therefore, the assemblies can form from attraction of particles over substantial distances. The technique should also be applicable to other charged species, such as properly derivatized nanoparticles. In the example of the charged gold disks, the assemblies lack in-plane ordering, presumably because they lack surface mobility once they absorb. Therefore, if in-plane ordering is required, other features must be designed into the process to allow for equilibration and lateral ordering.[91] In addition, the current example only consists of a single layer of gold plates on a surface. Nevertheless, the process demonstrates the substantial possibilities offered by the electrostatic assembly technique for enabling the control of in-plane deposition in a variety of monolayer and multilayer configurations.

V. Evaporation Techniques

In some cases, solvent techniques are not appropriate for the deposition of hybrid films. Some applications or studies also require deposition under vacuum conditions. The problem with evaporating the hybrid materials is that the organic component of the structure will generally dissociate or decompose from the material at substantially lower temperatures, or in a shorter time interval, relative to the inorganic component. Therefore, if a source containing the hybrid is gradually heated in a vacuum chamber, the deposited films will not, in general, consist of the same hybrid as the initial source. Two broad approaches have been employed to overcome this thermal or temporal incompatibility between the organic and inorganic components during evaporation.

Multiple Source. In two-source thermal evaporation, a separate source is utilized for the organic and inorganic components, thereby enabling the use of different power conditions for the two components. An interesting example of this is the creation of copper phthalocyanine (CuPc)/TiO_x multilayers by thermal evaporation, using a multi-ion source type ICB deposition apparatus contained within a vacuum environment.[2] A tungsten crucible for CuPc and a graphite crucible for Ti were separately heated to maintain an evaporation rate of 1 Å/s for each. Alternating layers were fabricated by using shutters for each crucible while monitoring the film growth with an oscillating quartz crystal thickness monitor. The targeted periodicity ranged from 50 to 400 Å. The substrate temperatures used for the deposition (~200 °C) yielded nominally amorphous TiO_x layers, whereas interfacial roughness in the artificial multilayers was less than 30 Å (i.e., still a significant fraction of the targeted periodicity). The resulting multilayer structures exhibited photoconductivities that were significantly larger than that observed in comparable single layers of CuPc, presumably because of the greater probability of charge separation at the organic−inorganic interface.[2]

Artificial 8-hydroxyquinoline aluminum (Alq)/MgF_2 multilayer structures have also been created using similar techniques to that described above for the CuPc/TiO_x structures, with Alq layer thickness varying between 10 and 50 Å and the MgF_2 layer thickness held constant at 30 Å.[92] Alq was chosen for its fluorescence and stability, whereas MgF_2 is a low refractive index material having a wide transmission region from 200 to 5000 nm. Interfacial roughness in these films was observed to be much smaller than 10 Å. Changes in the Alq exciton energy in absorption and photoluminescence measurements, as a function of Alq layer thickness, were interpreted as quantum confinement effects of the exciton in the organic layer. Similar artificial hybrid multilayer structures based on phthalocyanato tin(IV) dichloride ($SnCl_2Pc$)/cadmium(II) selenide[93] and CuPc/PbTe[94] (in this case deposited using a combination of thermal evaporation and pulsed laser deposition) have also been developed.

Note that in the artificially prepared hybrid multilayer structures interfacial roughness between layers

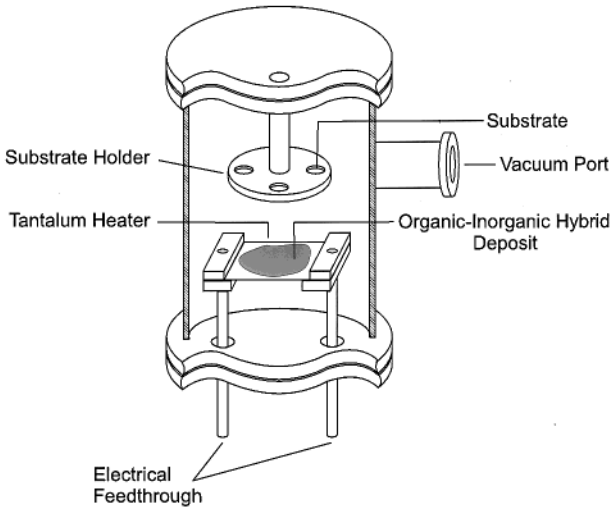

Figure 9. Schematic cross section of a single source thermal ablation chamber.[96]

can impede the observation of expected superlattice effects and limit the lower end of achievable thickness for the component layers. The self-assembling hybrid perovskites (and related materials) provide an opportunity for the creation of superlattice structures with atomically smooth interfaces and very small dimensions. In the $(R-NH_3)_2MX_4$ (M = Sn or Pb; X = Cl, Br, or I) perovskite systems, for example, single crystals can be grown with 6 Å wide wells and barrier widths that are controlled by the length of the R-group. Varying the number of perovskite layers between the organic bilayers in the series $(R-NH_3)_2(CH_3NH_3)_{n-1}M_nI_{3n+1}$ also enables control over the well width. Films of the lead(II)-iodide-based members of this series, $(C_6H_5C_2H_4NH_3)_2PbI_4$ and $(CH_3NH_3)PbI_3$, have been successfully created using a two source thermal evaporation process.[95] For the phenethylammonium compound, PbI_2 and $C_6H_5C_2H_4NH_2{\cdot}HI$ were simultaneously deposited onto a fused quartz substrate under a base pressure of $\sim 10^{-6}$ Torr. During the deposition, the substrates were allowed to remain at room temperature. The resulting films demonstrated the characteristic absorption spectrum and X-ray pattern for the hybrid perovskite. Film growth is proposed to occur through the intercalation of organic ammonium iodide into the simultaneously deposited PbI_2 film. The previously discussed (section III) demonstration that hybrid perovskite films can be formed through the vapor-phase intercalation of alkylammonium bromide into predeposited lead(II) bromide films provides further support for this mechanism.[45]

Single Source. Although the metal halide component of the hybrid evaporates in a well-defined fashion in the two-source process, the organic salt deposition is often difficult to control. In addition, given the relatively long times required for evaporation, high vacuum conditions are required during these depositions. Recently, a single source thermal ablation (SSTA) technique has been reported[96] that employs a single evaporation source and very rapid heating.

The prototype single source thermal ablation (SSTA) apparatus (Figure 9) consists of a vacuum chamber, with an electrical feed-through to a thin tantalum sheet heater.[96] The starting charge is deposited on the heater in the form of crystals, powder, or a concentrated solution (which is allowed to dry before ablating). Insoluble powders are ideally placed on the heater in the form of a suspension (in a quick-drying solvent), because this enables the powder to be in better physical and thermal contact with, as well as more evenly dispersed across, the sheet. After establishing a suitable vacuum, a large current is passed through the heater. While the sheet temperature reaches approximately 1000 °C in 1−2 s, the entire starting charge ablates from the heater surface well before it incandesces. The organic and inorganic components reassemble on the substrates (positioned above the tantalum sheet) after ablation to produce optically clear films of the desired product. The key aspect to this process is that the ablation is quick enough for the organic and inorganic components to leave the source at essentially the same time and before the organic component has had a chance to decompose. In many cases (especially with relatively simple organic cations), the as-deposited films are single phase and crystalline, indicating that the organic−inorganic hybrids can reassemble on the substrate at room temperature.

A number of organic−inorganic hybrids have been deposited using this technique, including $(C_6H_5C_2H_4NH_3)_2PbBr_4$, $(C_6H_5C_2H_4NH_3)_2PbI_4$, $(C_4H_9NH_3)_2SnI_4$, as well as $(C_4H_9NH_3)_2(CH_3NH_3)Sn_2I_7$.[96] The successful deposition of $(C_4H_9NH_3)_2(CH_3NH_3)Sn_2I_7$ films demonstrates that mixed-organic-cation systems can be deposited. For each compound, approximately 15 mg of the organic−inorganic perovskite is dissolved in 1 mL of anhydrous *N*,*N*-dimethylformamide (DMF) or methanol. For $(C_6H_5C_2H_4NH_3)_2PbBr_4$ and $(C_4H_9NH_3)_2SnI_4$, the best results are achieved using a stoichiometric starting solution. For $(C_6H_5C_2H_4NH_3)_2PbI_4$, however, better results are achieved by including a small excess of phenethylammonium iodide in the initial solution. A small volume of the solution is dried on the tantalum foil. After pumping the chamber to $<10^{-4}$ Torr, the vacuum valve is closed and a large current is passed through the heater for several seconds, ablating the hybrid from the tantalum foil. The initial volume of material placed on the heater determines the resulting film thickness deposited on the substrate (generally, 10 to >200 nm). An atomic force microscope (AFM) study of an as-prepared (i.e., unannealed) $(C_6H_5C_2H_4NH_3)_2PbI_4$ film demonstrates a mean roughness of approximately 1.6 nm, similar to the values observed for spin-coated films of the same material. The thermally ablated films also exhibit a relatively small (<75 nm) grain size. X-ray diffraction patterns (Figure 10) demonstrate that the as-deposited films are single phase, crystalline, and highly oriented (as for spin-coated films of the same material).

Deposition of crystalline organic−inorganic perovskite films with more complex organic cations sometimes requires a short (∼15 min) low-temperature (<250 °C) postdeposition anneal. Films of $(H_2AETH)PbX_4$ {X = Br or I; AETH = 1,6-bis[5′-(2″-aminoethyl)-2′-thienyl]hexane}, for example, have been deposited using the SSTA technique.[97] However, the as-deposited films do not exhibit a diffraction pattern, indicating the very fine-grained or amorphous nature of the films. Low-temperature annealing leads to progressive grain growth (as observed in X-ray diffraction patterns and AFM studies)

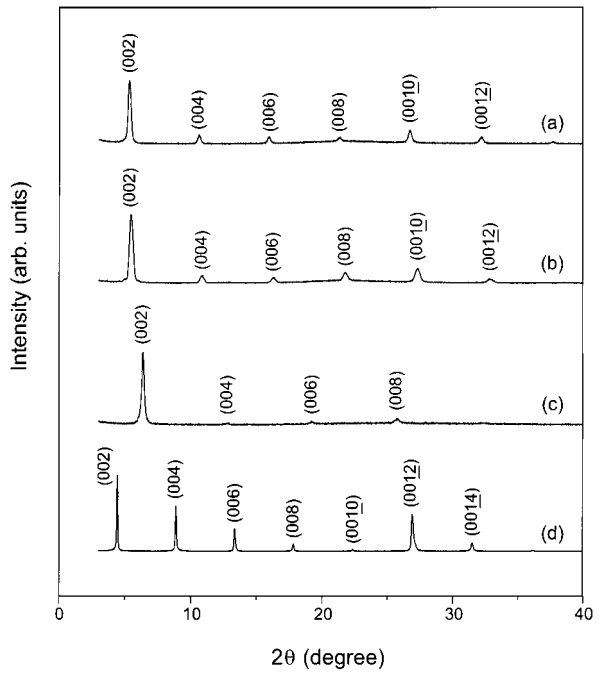

Figure 10. Room-temperature X-ray diffraction data for unannealed SSTA-deposited films of the organic−inorganic perovskites (a) $(C_6H_5C_2H_4NH_3)_2PbBr_4$, (b) $(C_6H_5C_2H_4NH_3)_2PbI_4$, (c) $(C_4H_9NH_3)_2SnI_4$, and (d) $(C_4H_9NH_3)_2(CH_3NH_3)Sn_2I_7$.[96]

and a bathochromic shift of the characteristic perovskite layer exciton peak in the absorption data. For the $(H_2AETH)PbI_4$ system, the optimal annealing condition for achieving a well-crystallized film is approximately 120 °C for 15 min. Heating much above this temperature leads to the decomposition of the organic component of the film, leaving behind PbI_2.

As seen from these examples, single source thermal ablation offers the ability to expeditiously produce high quality films, without the need to find a suitable solvent for the hybrid (one that both dissolves the hybrid and wets the substrate surface) or to balance deposition rates from multiple evaporation sources. The rapid nature of the ablation process enables a quick turnaround time and also relaxes the need for stringent vacuum conditions. The high quality of the resulting films and the ability to pattern the films during the deposition process suggests the applicability of the SSTA process for fabricating devices. LEDs incorporating SSTA-deposited $(H_2AEQT)PbCl_4$ [AEQT = 5,5‴-bis-(aminoethyl)-2,2′:5′,2″:5″,2‴-quaterthiophene] exhibit srong electroluminescence at room temperature.[14]

VI. Conclusion

Although single crystals are generally the most useful medium for examining structural and physical properties of organic−inorganic hybrids, many applications and some measurements require the ability to deposit thin films. A number of new techniques, as well as modifications of established processes, have been designed to deposit hybrid materials on a variety of substrates. These include sol−gel based deposition and other solution-based techniques, intercalation reactions, layer-by-layer assembly, and evaporation-based techniques. A number of examples of each type of deposition have been given in this review. It should be noted, however, that there has been great interest in hybrid films over the last 10 years (as evidenced by the long list of references given below). Consequently, the presented examples are meant to be representative of each technique, rather than an exhaustive list of all recent progress. In addition, no attempt has been made to cover the important area of characterization techniques for the hybrid films. Measurement of thickness, homogeneity, topology, periodicity, and composition are all very important aspects to consider,[98] and the hybrids present special challenges with respect to these characterizations. For example, examination of organic−inorganic hybrids under a scanning-electron microscope (SEM) can be complicated by the instability of the organic component with respect to electron bombardment (without special precautions).

Organic−inorganic hybrids provide many new possibilities for materials synthesis since they can combine useful attributes of organic and inorganic materials within a single molecular scale composite. Numerous examples of this have been presented throughout this review. However, one typical class of examples include sol−gel-derived or self-assembled nonlinear optical materials, where the organic component is a highly polarizable dye and the inorganic component provides the structural and thermal stability holding the dye molecules in a polar configuration.[31,32,67,70,71] The hybrids also present opportunities for ordering solids on a number of different length scales (i.e., possibility of hierarchical organization). For example, hybrids can be designed based on molecular components, as well as on preformed nanoparticles and polyelectrolytes of various forms and sizes (e.g., exfoliated clays, polymers, and charged metal disks). As in biological organic−inorganic hybrids (e.g., sea shell, tooth enamel, and bone),[99] the organic component can template the formation of the inorganic framework, and conversely, the inorganic framework can influence the bonding and conformation of the organic component.[100] A variety of different types of connections between the two components of the hybrid also enable a degree of control over the communication between the organic and inorganic entities. Included among these interactions are hydrogen bonding, ionic and covalent bonding, and van der Waals interaction.

Finally, the thin film techniques described in this review not only provide a means of depositing known or thermodynamically stable hybrids, but also enable the creation of hybrids that cannot readily be stabilized in bulk form. The layer-by-layer techniques (both solution and evaporation-based) are particularly important in this regard because monolayer control of stoichiometry, structure, and functionality can in principle be exerted. Of recent interest is the possibility of using self-assembly to control the ordering of molecules, both between layers and within the layers that make up the multilayered structure.[91] The solution-based techniques (e.g., stamping and spin-coating) are also particularly attractive because of the simplicity of the processes, as well as the low temperatures at which the depositions occurs. The low temperatures enable thin film formation on a wide range of temperature-sensitive substrates, including flexible plastics. The resulting hybrid films are expected to provide numerous exciting opportunities

for organic−inorganic electronics,[41] as well as for more basic scientific exploration.

Acknowledgment. The author gratefully acknowledges the fruitful collaborations that have contributed to his knowledge of hybrid thin films, including work with K. Liang, K. Chondroudis, L. Kosbar, and M. Prikas.

References

(1) Sakata, T.; Hashimoto, K.; Hiramoto, M. *J. Phys. Chem.* **1990**, *94*, 3040.
(2) Takada, J.; Awaji, H.; Koshioka, M.; Nakajima, A.; Nevin, W. A. *Appl. Phys. Lett.* **1992**, *61*, 2184.
(3) Miyasaka, T.; Watanabe, T.; Fujishima, A.; Honda, K. *J. Am. Chem. Soc.* **1978**, *100*, 6657.
(4) Hong, X.; Ishihara, T.; Nurmikko, A. V. *Phys. Rev. B* **1992**, *45*, 6961.
(5) For a review, see: Mitzi, D. B. *Prog. Inorg. Chem.* **1999**, *48*, 1.
(6) Mitzi, D. B.; Feild, C. A.; Harrison, W. T. A.; Guloy, A. M. *Nature* **1994**, *369*, 467.
(7) Mitzi, D. B.; Wang, S.; Feild, C. A.; Chess, C. A.; Guloy, A. M. *Science* **1995**, *267*, 1473.
(8) Ishihara, T.; Takahashi, J.; Goto, T. *Solid State Commun.* **1989**, *69*, 933.
(9) Papavassiliou, G. C.; Koutselas, I. B. *Synth. Met.* **1995**, *71*, 1713.
(10) Calabrese, J.; Jones, N. L.; Harlow, R. L.; Herron, N.; Thorn, D. L.; Wang, Y. *J. Am. Chem. Soc.* **1991**, *113*, 2328.
(11) Fujita, T.; Sato, Y.; Kuitani, T.; Ishihara, T. *Phys. Rev. B* **1998**, *57*, 12428.
(12) Era, M.; Morimoto, S.; Tsutsui, T.; Saito, S. *Appl. Phys. Lett.* **1994**, *65*, 676.
(13) Mitzi, D. B.; Chondroudis, K.; Kagan, C. R. *Inorg. Chem.* **1999**, *38*, 6246.
(14) Chondroudis, K.; Mitzi, D. B. *Chem. Mater.* **1999**, *11*, 3028.
(15) (a) Chondroudis, K.; Dimitrakopoulos, C. D.; Mitzi, D. B. Unpublished work, 1998. (b) Chondroudis, K.; Dimitrakopoulos, C. D.; Kagan, C. R.; Kymissis, I.; Mitzi, D. B. U.S. Patent 6,-180,956, January 30, 2001.
(16) Kagan, C. R.; Mitzi, D. B.; Dimitrakopoulos, C. D. *Science* **1999**, *286*, 945.
(17) Mitzi, D. B.; Dimitrakopoulos, C. D.; Kosbar, L. *Chem. Mater.* **2001**, *13*, 3728.
(18) (a) Gamble, F. R.; DiSalvo, F. J.; Klemm, R. A.; Geballe, T. H. *Science* **1970**, *168*, 568. (b) Parkin, S. S. P.; Engler, E. M.; Schumaker, R. R.; Lagier, R.; Lee, V. Y.; Scott, J. C.; Greene, R. L. *Phys. Rev. Lett.* **1983**, *50*, 270.
(19) Lacroix, P. G.; Clément, R.; Nakatani, K.; Zyss, J.; Ledoux, I. *Science* **1994**, *263*, 658.
(20) Cao, G.; Garcia, M. E.; Alcalá, M.; Burgess, L. F.; Mallouk, T. E. *J. Am. Chem. Soc.* **1992**, *114*, 7574.
(21) Jones, R. W. *Fundamental Principles of Sol−Gel Technology*; The Institute of Metals: London, 1989.
(22) Schmidt, H. *J. Non-Cryst. Solids* **1985**, *73*, 681.
(23) Wilkes, G. L.; Orler, B.; Huang, H.-H. *Polym. Prepr.* **1985**, *26*, 300.
(24) Sorek, Y.; Reisfeld, R.; Weiss, A. M. *Chem. Phys. Lett.* **1995**, *244*, 371.
(25) Novak, B. M. *Adv. Mater.* **1993**, *5*, 422.
(26) Jang, S. H.; Han, M. G.; Im, S. S. *Synth. Met.* **2000**, *110*, 17.
(27) Chen, Y.; Iroh, J. O. *Chem. Mater.* **1999**, *11*, 1218.
(28) Prosposito, P.; Casalboni, M.; De Matteis, F.; Pizzoferrato, R. *Thin Solid Films* **2000**, *373*, 150.
(29) Sorek, Y.; Reisfeld, R.; Weiss, A. M. *Chem. Phys. Lett.* **1995**, *244*, 371.
(30) Keum, J. H.; Kang, E.; Kim, Y.; Cho, W. J.; Ha, C. S. *Mol. Cryst. Liq. Cryst.* **1998**, *316*, 297.
(31) Hayakawa, T.; Imaizumi, D.; Nogami, M. *J. Mater. Res.* **2000**, *15*, 530.
(32) Kang, S.-J.; Choi, S.-K.; Lee, H.-J.; Lee, J.-H.; Kim, H. K. *Nonlinear Opt.* **1996**, *15*, 181.
(33) Roscher, C.; Buestrich, R.; Dannberg, P.; Rösch, O.; Popall, M. *Mater. Res. Symp. Proc.* **1998**, *519*, 239.
(34) Sorek, Y.; Reisfeld, R.; Finkelstein, I.; Ruschin, S. *Appl. Phys. Lett.* **1995**, *66*, 1169.
(35) Finkelstein, I.; Ruschin, S.; Sorek, Y.; Reisfeld, R. *Opt. Mater.* **1997**, *7*, 9.
(36) Kresge, C. T.; Leonowicz, M. E.; Vartuli, J. C.; Beck, J. S. *Nature* **1992**, *359*, 710.
(37) Zhou, H. S.; Honma, I. *Mater. Res. Soc. Symp. Proc.* **1998**, *519*, 77.
(38) Sellinger, A.; Weiss, P. M.; Nguyen, A.; Lu, Y.; Assink, R. A.; Brinker, C. J. *Mater. Res. Soc. Symp. Proc.* **1998**, *519*, 95.
(39) Ishihara, T. In *Optical Properties of Low-Dimensional Materials*, Ogawa, T., Kanemitsu, Y., Eds., World Scientific: Singapore, 1995; pp 288−339.
(40) Kitazawa, N. *Mater. Sci. Eng.* **1997**, *B49*, 233.
(41) Mitzi, D. B.; Chondroudis, K.; Kagan, C. R. *IBM J. Res. Dev.* **2001**, *45*, 29.
(42) Liang, K.; Mitzi, D. B.; Prikas, M. T. *Chem. Mater.* **1998**, *10*, 403.
(43) Kitazawa, N. *J. Mater. Sci.* **1998**, *33*, 1441.
(44) Kato, T.; Suzuki, T.; Irie, T. *Chem. Lett.* **2000**, *2*, 186.
(45) Era, M.; Kakiyama, N.; Ano, T.; Nagano, M. *Trans. Mater. Res. Soc. Jpn.* **1999**, *24*, 509.
(46) (a) Blodgett, K. B. *J. Am. Chem. Soc.* **1935**, *57*, 1007. (b) Blodgett, K. B.; Langmuir, I. *Phys. Rev.* **1937**, *51*, 964.
(47) Petty, M. C. *Langmuir−Blodgett Films−An Introduction*; Cambridge University Press: Cambridge, U.K., 1996.
(48) See, for example, (a) Clearfield, A. *Comments Inorg. Chem.* **1990**, *10*, 89. (b) Cao, G.; Lee, H.; Lynch, V. M.; Mallouk, T. E. *Inorg. Chem.* **1988**, *27*, 2781.
(49) Seip, C. T.; Granroth, G. E.; Meisel, M. W.; Talham, D. R. *J. Am. Chem. Soc.* **1997**, *119*, 7084.
(50) Mingotaud, C.; Lafuente, C.; Gomez-Garcia, C.; Ravaine, S.; Delhaes, P. *Mol. Cryst. Liq. Cryst.* **1999**, *335*, 349.
(51) Petruska, M. A.; Talham, D. R. *Chem. Mater.* **1998**, *10*, 3672.
(52) Petruska, M. A.; Talham, D. R. *Langmuir* **2000**, *16*, 5123.
(53) Wu, A.; Talham, D. R. *Langmuir* **2000**, *16*, 7449.
(54) Era, M.; Oka, S. *Thin Solid Films* **2000**, *376*, 232.
(55) Clemente-León, M.; Agricole, B.; Mingotaud, C.; Gómez-García, C. J.; Coronado, E.; Delhaes, P. *Langmuir* **1997**, *13*, 2340.
(56) Keggin, J. F. *Nature* **1933**, *131*, 908.
(57) Gómez-García, C. J.; Giménez-Saiz, C.; Triki, S.; Coronado, E.; Le Magueres, P.; Ouahab, L.; Ducasse, L.; Sourisseau, C.; Delhaes, P. *Inorg. Chem.* **1995**, *34*, 4139.
(58) Tamura, K.; Setsuda, H.; Taniguchi, M.; Takahashi, M.; Yamagishi, A. *Clay Sci.* **1998**, *10*, 409.
(59) Taguchi, Y.; Kimura, R.; Azumi, R.; Tachibana, H.; Koshizaki, N.; Shimomura, M.; Momozawa, N.; Sakai, H.; Abe, M.; Matsumoto, M. *Langmuir* **1998**, *14*, 6550.
(60) Ulman, A. *An Introduction to Ultrathin Organic Films From Langmuir−Blodgett to Self-Assembly*; Academic Press: San Diego, CA, 1991.
(61) Netzer, L.; Sagiv, J. *J. Am. Chem. Soc.* **1983**, *105*, 674.
(62) Tillman, N.; Ulman, A.; Penner, T. L. *Langmuir* **1989**, *5*, 101.
(63) Li, D.; Ratner, M. A.; Marks, T. J.; Zhang, C.; Yang, J.; Wong, G. K. *J. Am. Chem. Soc.* **1990**, *112*, 7389.
(64) Lee, H.; Kepley, L. J.; Hong, H.-G.; Mallouk, T. E. *J. Am. Chem. Soc.* **1988**, *110*, 618.
(65) Cao, G.; Hong, H.-G.; Mallouk, T. E. *Acc. Chem. Res.* **1992**, *25*, 420.
(66) Dines, M. B.; DiGiacomo, P. M. *Inorg. Chem.* **1981**, *20*, 92.
(67) Katz, H. E.; Scheller, G.; Putvinski, T. M.; Schilling, M. L.; Wilson, W. L.; Chidsey, C. E. D. *Science* **1991**, *254*, 1485.
(68) Neff, G. A.; Mahon, T. M.; Abshere, T. A.; Page, C. J. *Mater. Res. Soc. Symp. Proc.* **1996**, *435*, 661.
(69) Neff, G. A.; Page, C. J.; Meintjes, E.; Tsuda, T.; Pilgrim, W.-C.; Roberts, N.; Warren, W. W., Jr. *Langmuir* **1996**, *12*, 238.
(70) Ungashe, S. B.; Wilson, W. L.; Katz, H. E.; Scheller, G. R.; Putvinski, T. M. *J. Am. Chem. Soc.* **1992**, *114*, 8717.
(71) Byrd, H.; Suponeva, E. P.; Bocarsly, A. B.; Thompson, M. E. *Nature* **1996**, *380*, 610.
(72) (a) Ansell, M. A.; Zeppenfeld, A. C.; Yoshimoto, K.; Cogan, E. B.; Page, C. J. *Chem. Mater.* **1996**, *8*, 591. (b) Ansell, M. A.; Cogan, E. B.; Page, C. J. *Langmuir* **2000**, *16*, 1172.
(73) (a) Bohling, D. A.; Mann, K. R. *Inorg. Chem.* **1983**, *22*, 1561. (b) Bohling, D. A.; Mann, K. R. *Inorg. Chem.* **1984**, *23*, 1426.
(74) Bell, C. M.; Arendt, M. F.; Gomez, L.; Schmehl, R. H.; Mallouk, T. E. *J. Am. Chem. Soc.* **1994**, *116*, 8374.
(75) Bell, C. M.; Keller, S. W.; Lynch, V. M.; Mallouk, T. E. *Mater. Chem. Phys.* **1993**, *35*, 225.
(76) Hao, E.; Wang, L.; Zhang, J.; Yang, B.; Zhang, X.; Shen, J. *Chem. Lett.* **1999**, *1*, 5.
(77) Iler, R. K. *J. Colloid Interface Sci.* **1966**, *21*, 569.
(78) Kleinfeld, E. R.; Ferguson, G. S. *Science* **1994**, *265*, 370.
(79) Kleinfeld, E. R.; Ferguson, G. S. *Chem. Mater.* **1996**, *8*, 1575.
(80) Kotov, N. A.; Haraszti, T.; Turi, L.; Zavala, G.; Geer, R. E.; Dékány, I.; Fendler, J. H. *J. Am. Chem. Soc.* **1997**, *119*, 6821.
(81) Kleinfeld, E. R.; Ferguson, G. S. *Chem. Mater.* **1995**, *7*, 2327.
(82) Kotov, N. A.; Magonov, S.; Tropsha, E. *Chem. Mater.* **1998**, *10*, 886.
(83) Kotov, N. A.; Dékány, I.; Fendler, J. H. *Adv. Mater.* **1996**, *8*, 637.
(84) Gao, M.; Richter, B.; Kirstein, S.; Möhwald, H. *J. Phys. Chem. B* **1998**, *102*, 4096.
(85) Colvin, V. L.; Schlamp, M. C.; Alivisatos, A. P. *Nature* **1994**, *370*, 354.
(86) Cassagneau, T.; Mallouk, T. E.; Fendler, J. H. *J. Am. Chem. Soc.* **1998**, *120*, 7848.
(87) Gao, M.; Gao, M.; Zhang, X.; Yang, Y.; Yang, B.; Shen, J. *J. Chem. Soc., Chem. Commun.* **1994**, 2777.
(88) Liu, Y.; Wang, A.; Claus, R. *J. Phys. Chem. B* **1997**, *101*, 1385.

(89) Schmitt, J.; Decher, G.; Dressick, W. J.; Brandow, S. L.; Geer, R. E.; Shashidhar, R.; Calvert, J. M. *Adv. Mater.* **1997**, *9*, 61.
(90) Aliev, F. G.; Correa-Duarte, M. A.; Mamedov, A.; Ostrander, J. W.; Giersig, M.; Liz-Marzán, L. M.; Kotov, N. A. *Adv. Mater.* **1999**, *11*, 1006.
(91) Tien, J.; Terfort, A.; Whiteside, G. M. *Langmuir* **1997**, *13*, 5349.
(92) Tokito, S.; Sakata, J.; Taga, Y. *Appl. Phys. Lett.* **1994**, *64*, 1353.
(93) Imanishi, Y.; Ishihara, S.; Hamada, T. *Mol. Cryst. Liq. Cryst.* **1998**, *315*, 111.
(94) Lee, H.; Kang, Y.; Choi, B.; Jeong, J.; Tabata, H.; Kawai, T. *J. Korean Phys. Soc.* **1999**, *34*, S64.
(95) Era, M.; Hattori, T.; Taira, T.; Tsutsui, T. *Chem. Mater.* **1997**, *9*, 8.
(96) Mitzi, D. B.; Prikas, M. T.; Chondroudis, K. *Chem. Mater.* **1999**, *11*, 542.
(97) Chondroudis, K.; Mitzi, D. B.; Brock, P. *Chem. Mater.* **2000**, *12*, 169.
(98) A brief discussion of these techniques is included in Cassagneau, T. P.; Sweryda-Krawiec, B.; Fendler, J. H. *MRS Bulletin* **2000**, *25 (*No. 9), 40.
(99) (a) Lowenstam, H. A.; Weiner, S. *On Biomineralization*; Oxford University Press: New York, 1989. (b) Currey, J. D. *J. Mater. Educ.* **1987**, *9*, 120.
(100) Mitzi, D. B. *J. Chem. Soc., Dalton Trans.* **2001**, 1.

CM0101677